Comparing *F* region ionospheric irregularity observations from C/NOFS and Jicamarca

D. L. Hysell,[1] R. B. Hedden,[1] J. L. Chau,[2] F. R. Galindo,[2] P. A. Roddy,[3] and R. F. Pfaff[4]

Received 1 May 2009; revised 2 June 2009; accepted 8 June 2009; published 11 July 2009.

[1] Observations of plasma density irregularities associated with equatorial spread *F* (ESF) have been made using the Jicamarca Radio Observatory and the Plasma Langmuir Probe (PLP) and Vector Electric Field Instrument (VEFI) instruments on the Communications Navigation Outage Forecast System (C/NOFS) satellite during a close spatio-temporal conjunction. The radar data resolution is of the order of 1 km and a few sec. in space and time, respectively. We find that coherent scatter intensifications at these scales are coincident and collocated with plasma density depletions as determined by C/NOFS. The Doppler shifts of the localized echoes are also comparable to the vertical components of the $\mathbf{E} \times \mathbf{B}$ plasma drifts. The strongest backscatter does not necessarily come from the deepest or most rapidly convecting depletions. This implies a complex relationship between coherent backscatter and the underlying state parameters in the ionospheric plasma. **Citation:** Hysell, D. L., R. B. Hedden, J. L. Chau, F. R. Galindo, P. A. Roddy, and R. F. Pfaff (2009), Comparing *F* region ionospheric irregularity observations from C/NOFS and Jicamarca, *Geophys. Res. Lett.*, *36*, L00C01, doi:10.1029/2009GL038983.

1. Introduction

[2] In a recent review paper, *Woodman* [2009] documents steady progress toward a comprehensive picture of ionospheric plasma irregularities in equatorial spread *F* (ESF). Theory followed experimental results from satellites, sounding rockets, ground-based radars, and other radio frequency apparatus. Observations of meter-scale plasma density irregularities in ESF from coherent scatter radars have played a crucial role [e.g., *Woodman and La Hoz*, 1976; *Hysell and Burcham*, 1998; *Yokoyama et al.*, 2004; *de Paula and Hysell*, 2004; *Patra et al.*, 2004; *Otsuka et al.*, 2004; *Tsunoda and Ecklund*, 2007]. By assuming that the meter-scale irregularities serve as tracers of intermediate- and large-scale dynamics, radar scientists have elucidated the plasma instability processes underlying ESF and also documented the morphological characteristics, seasonal dependencies, and space weather impacts of the phenomenon.

[3] A fundamental, unresolved question is the relationship between the meter-scale irregularities detected by coherent scatter radars to the underlying state parameters of the ionospheric plasma. How are the coherent scatter echoes related to plasma density and drifts, and in what precise sense do they serve as tracers?

[4] *Kelley et al.* [1976] were the first to experimentally relate plasma depletions observed by sounding rockets with coherent backscatter, but precisely connecting the two phenomena in space and time was impractical using radar equipment and techniques available at the time. *Morse et al.* [1977] associated coherent backscatter seen at Jicamarca with steep vertical plasma density gradients observed by sounding rockets but were forced to assume that the irregularities were frozen into a uniform background flow to make the association. Similar remarks hold for subsequent experiments combining spacecraft with fixed-beam radars [e.g., *Kelley et al.*, 1986; *Pfaff et al.*, 1997].

[5] *Rino et al.* [1981] exploited the fully steerable Altair radar on Kwajalein Atoll to observe ESF plasma irregularities during the PLUMEX I rocket experiment. The collocation/coincidence of the rocket and radar measurements was relatively precise compared to earlier experiments and confirmed that coherent backscatter arose from regions of plasma structuring where the mean density was well below background. Similar results were obtained by *Tsunoda et al.* [1982] comparing Altair radar data to plasma density profiles measured by the AE-E satellite. In both cases, the precision of the association was limited by the radar pulsing mode, incoherent integration time, beamwidth, and pointing slew rate of the radar together with the finite speed of the spacecraft in a complicated way. The actual degree of collocation/coincidence appears to have been a few tens of kilometers in space and a few tens of seconds in time. However, radar imaging experiments conducted at Jicamarca have shown that the coherent scatter from ESF is spatially intermittent and composed of backscatter from compact regions of space typically no more than a few kilometers in dimension [e.g., *Hysell*, 1998].

[6] A rigorous theoretical solution to the problem of meter-scale irregularities in ESF necessitates the treatment of both kinetic and nonlinear effects as well as phenomena at both small and large scales and remains elusive. *Huba and Ossakow* [1979, 1981] advanced theories for the generation of meter- and sub meter-scale irregularities based on kinetic drift wave and lower hybrid drift wave theories, respectively. Using fluid theory, *Hysell* [1998] associated the meter-scale waves with vertically steepened structures at the leading edges of convecting, kilometer-scale plasma depletions and enhancements [see also *Costa and Kelley*, 1978]. They predicted that the enhanced backscatter should

[1]Department of Earth and Atmospheric Sciences, Cornell University, Ithaca, New York, USA.
[2]Jicamarca Radio Observatory, Geophysical Institute of Peru, Lima, Peru.
[3]Space Vehicles Directorate, Air Force Research Laboratory, Hanscom AFB, Massachusetts, USA.
[4]NASA Goddard Space Flight Center, Greenbelt, Maryland, USA.

0094-8276/09/2009GL038983$05.00

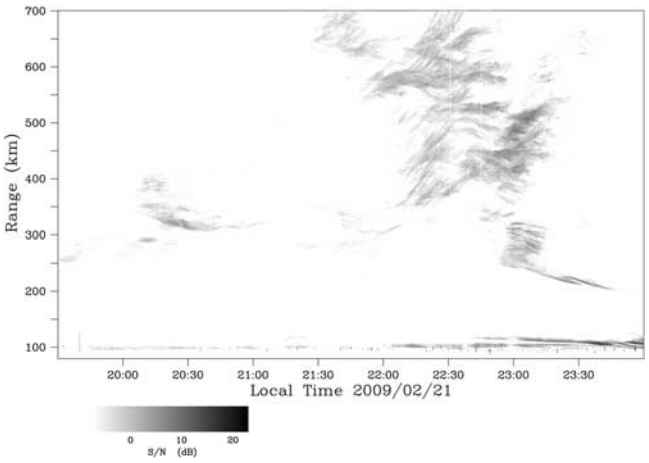

Figure 1. Range time intensity representation of coherent backscatter from ionospheric irregularities on Feb. 21, 2009. Grayscales represent signal-to-noise ratio in dB. The C/NOFS satellite passed near Jicamarca at about 2237 LT, 420 km altitude (see text).

be seen in the immediate horizontal centers of the kilometer-scale density irregularities and that the Doppler shifts should be related to the plasma convection speed within them but not necessarily to the bulk $\mathbf{E} \times \mathbf{B}$ drift velocity.

[7] We revisit the problem of combined radar and spacecraft observations of plasma irregularities in ESF. Using aperture synthesis imaging techniques, we measure coherent backscatter at Jicamarca with spatial and temporal resolution of the order of one kilometer and a few seconds, respectively. Such observations were made recently during conjunctions with the Air Force Communications Navigation Outage Forecast System (C/NOFS) satellite.

2. Observations

[8] Jicamarca was run on the evenings of Feb. 18–21, 2009, from approximately 1930–2400 LT in support of C/NOFS satellite passes. (Note that these are LT dates, and since UT = LT + 5 hr at Jicamarca, the corresponding UT dates are Feb. 19–22.) During this interval, the satellite passed through Jicamarca's longitude sector within about 1° of latitude. Note that potential structures in the plasma with transverse scale sizes of hundreds of meters are greater should be invariant over this translational span. The passes also occurred near perigee. These conditions permit the most unambiguous comparison of ground-based and in situ measurements of ionospheric irregularities. The advantage of perigee observations is that radar echoes from the lowest altitudes suffer the least degradation due to ionospheric scintillation. Scintillation effects at 50 MHz can be severe even during solar minimum [*Woodman*, 1960].

[9] Jicamarca was run in a new configuration for the experiments with closely interleaved coherent and incoherent scatter modes. The incoherent scatter results will be presented in another study. The coherent scatter mode was designed for aperture synthesis imaging, with uncoded short pulses transmitted on a single linear polarization of the east and west antenna quarters and with reception taking place on eight antenna modules displaced horizontally in space. These antennas afforded 28 distinct interferometry baselines, the longest being nearly 100 wavelengths long. A phase taper was applied to the transmitting antennas to broaden the transmitter antenna beam as much as possible. The range resolution for the imaging experiments was 300 m. The interpulse period for all experiments was 750 km, implying unambiguous Doppler frequency measurements between ±300 m/s.

[10] Figure 1 is a range-time-intensity plot of the coherent scatter received by Jicamarca on Feb. 21, 2009. The spread *F* event shown is dominated by several large, topside radar plumes that passed over the observatory between 2130–2330 LT. The echoes are relatively weak compared to those observed from plumes passing overhead immediately after sunset, and the absence of strong backscatter from the central channels of the plumes suggests that they had emerged hours before and drifted overhead later in their decay phase.

[11] In contrast, Figure 2 is a true radar image of the coherent backscatter received by Jicamarca at the precise moment of the C/NOFS satellite conjunction. The image was created using aperture synthesis techniques familiar in radio astronomy (see *Hysell and Chau* [2006] for a description of the algorithm). The pixels in the image are color coded according to the legend shown, with pixel brightness, hue, and saturation conveying information about the echo intensity, Doppler shift, and spectral width. Red (blue) shifted echoes are color coded red and blue, and positive (negative) velocities denote ascent (descent). Note that the transmitting antenna illuminated the central portion of the imaging domain only, although echoes can sometimes be seen at the periphery of the images inside the sidelobes. The angular resolution for the image is ∼0.1°, which corresponds to a zonal width of about 750 m at 425 km altitude. The incoherent integration time for the image is 4 seconds, approximately the transit time for the satellite through the radar illuminated beam.

[12] Despite having the appearance of so-called "dead bubbles" in Figure 1, the ionospheric irregularities in the radar images are actually dynamic, with Doppler shifts approaching 300 m/s in places and exhibiting considerable spatio-temporal variability (see auxiliary material).[1] Animated sequences of images like those in Figure 2 show that the turnover time for the largest features in the images is comparable to, or at least a significant fraction of, their transit time through the radar beam. Smaller features have correspondingly shorter turnover times. It would therefore be incorrect to invoke the frozen flow hypothesis in interpreting the observations. The backscatter is furthermore highly intermittent in space. Absent radar imaging, the radar observations would represent complicated spatial superposition of compact scatterers, even in the case of a narrow-beam radar like Jicamarca.

[13] Figure 2 is dominated by tilted features that we take to represent channels of depleted plasma penetrating through the *F* peak and into the topside under the action of generalized Rayleigh-Taylor instability. The westward tilt is usually attributed to the electrodynamics of vertically-elongated plasma depletions in the presence of horizontal neutral wind forcing but may also be influenced by varia-

[1] Auxiliary materials are available in the HTML. doi:10.1029/2009GL038983.

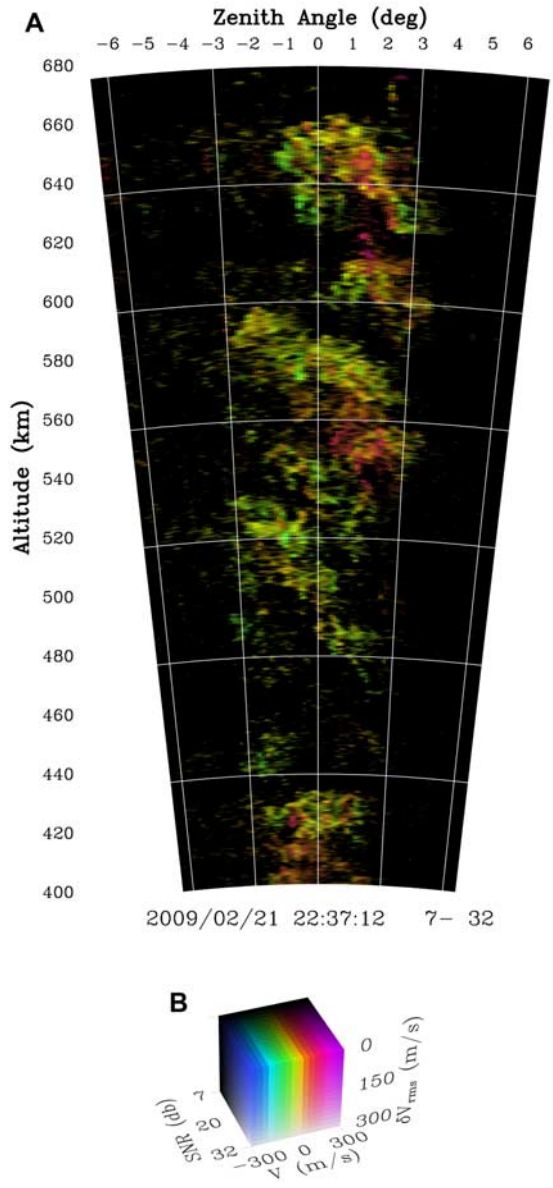

Figure 2. Radar image of coherent backscatter recorded during the C/NOFS satellite conjunction. Note that the aspect ratio of the figure is true. The right side of the image represents the eastern side.

tions in the flux-tube integrated conductivity and wind forcing terms with increasing apex altitude [e.g., *Zalesak et al.*, 1982; *Mendillo and Tyler*, 1983]. The westward edges of the depletion are further structured by secondary, wind-driven interchange instability, as noted by *Zalesak et al.* [1982] and *Tsunoda* [1983].

[14] Of greatest interest here are the irregularities near the bottom of Figure 2, the region probed by the C/NOFS satellite at perigee. The echoes here show relatively large Doppler shifts below about 420 km and small Doppler shifts above. Animated sequences of radar images suggest that the plasma was convecting upward rapidly below 420 km and advecting eastward above, the net effect being that of a clockwise-rotating vortex.

[15] Figure 3 shows an expanded view of the same radar image in Figure 2, this time plotted beneath plasma density data recorded by the Plasma Langmuir Probe (PLP) instrument aboard C/NOFS. The satellite and radar data are plotted such that their abscissas span the same range of longitudes. The midpoint time for the satellite data plot also matches the midpoint time of the incoherent integration interval for the radar image. The start and end times of the radar data integration correspond closely to the times when the satellite entered and exited the region illuminated by the radar. The altitude of the satellite, mapped along magnetic field lines to the volume probed by the radar, was precisely 424 km for the time interval shown.

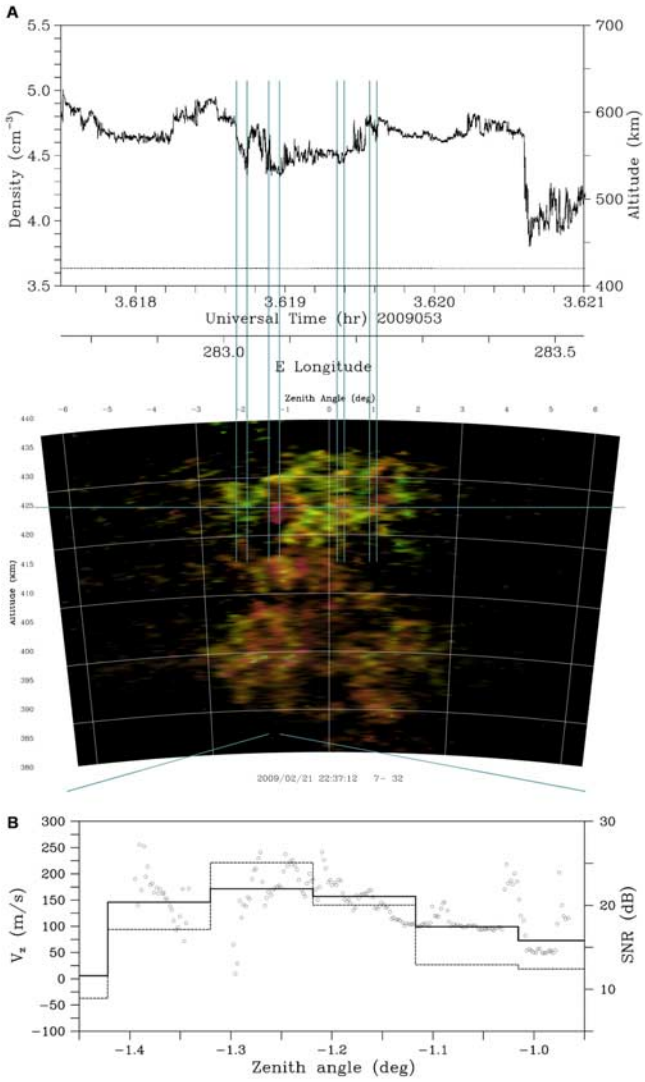

Figure 3. (a) Close-up view of the radar image from Figure 2. with C/NOFS satellite date plotted above on a logarithmic scale for comparison (see text). The aspect ratio of the radar image is true. Vertical lines highlight regions of enhanced backscatter at ∼424 km altitude. (b) Comparison of radar echoes and in situ electric field measurements made by the VEFI instrument on C/NOFS plotted on an expanded scale. Solid (dashed) lines represent the Doppler velocity and signal-to-noise ratio binned against zenith angle. Symbols represent vertical plasma drifts inferred from VEFI.

[16] The C/NOFS plasma density data presented here are from the Ion Trap sensor of the Planar Langmuir Probe instrument. The Ion Trap is conceptually similar to the Ion Velocity Meter (IVM) retarding potential analyzer flown on C/NOFS and other spacecraft in that it consist of a planar current collecting element behind a stack of biased metal grids. However, the Ion Trap has been optimized to measure ion density at rates up to 1 kHz. All Ion Trap measurements are initially made at 2 kHz. They are then processed by software-defined anti-alias filters before being averaged down to the telemetered data rate. The data here are all sampled at either 32 or 512 Hz rates. More details about the instrument are given by D. E. Hunton et al. (manuscript in preparation, 2009).

[17] Comparing the radar image to the PLP plasma density measurement, we find that bright spots in the image at about 424 km altitude correspond closely with density depletions within the resolution limits of the experiment. The bright spots in the images all persist for at least several frames and are not believed to be spurious. The most intense scattering regions are not necessarily the most deeply depleted ones, however. (For example, the brightest spot is the most eastward of the four highlighted.) Nor is it clear that the most deeply depleted regions give rise to backscatter with the largest Doppler shift. The most westward of the four depletions highlighted in Figure 3 is the most deeply depleted, but the echoes from this region appear to have small Doppler shifts.

[18] Electric field measurements on C/NOFS are available from the Vector Electric Field Experiment, VEFI, a three-axis double probe instrument that measures AC and DC electric fields and the associated $\mathbf{E} \times \mathbf{B}$ plasma drifts (R. F. Pfaff et al., manuscript in preparation, 2009). The double probes are formed using six rigid, 10-m booms that extend 11.8 cm diameter spherical sensors with embedded pre-amps, providing 20-m tip-to-tip baselines in three orthogonal directions. In addition, a DC fluxgate vector magnetometer provides accurate magnetic field information along the flight path to enable the $\mathbf{V} \times \mathbf{B}$ electric field contribution in the spacecraft frame to be calculated and subsequently removed from the measured potential differences.

[19] In order to examine the relationship between the Doppler shifts of the radar echoes and the electric fields measured in situ, we concentrate on the region at about $-1.25°$ zenith angle. Especially strong backscatter with large Doppler shifts indicative of rapid plasma ascent is evident here. Figure 3b compares the intensity and Doppler shift of the coherent scatter with the upward plasma $\mathbf{E} \times \mathbf{B}$ drifts measured by VEFI. The spatial resolution of the radar is coarse by comparison to the electric field measurements, which are sampled at a rate of 512 s^{-1}. The time registration is also a mismatch, since the satellite crossed the field of view covered by Figure 3 in less than 1 s. Qualifiers notwithstanding, the gross features in the radar and satellite drift measurements are comparable in the intensified scattering region examined here.

3. Analysis

[20] We have observed coherent scatter emerging mainly from regions where the plasma density observed by the C/NOFS satellite is structured and below background (localized depletions). This finding replicates the earlier results from the Altair radar [*Rino et al.*, 1981; *Tsunoda et al.*, 1982], except that the Altair data are coarsely resolved by comparison and likely represent aggregates of the scattering regions observed in the Jicamarca imaging experiments. Still finer resolution might reveal more fine structure, although spectral analysis of satellite data has shown that the scalar variance $\langle |\delta n|^2 \rangle$ decreases rapidly for scale sizes less than about one kilometer owing to the difficulty of supporting small-scale density fluctuations against diffusion [e.g., *Hysell and Kelley*, 1997]. More structure is anticipated at small scales in the electric fields, since the ambipolar field begins to dominate the polarization field at these scales.

[21] It follows that the apparent zonal motion of coherent scatter intensifications traces the advection of the localized depletions. In an incompressible flow, vertically-elongated density irregularities cannot overtake one-another as they drift horizontally and so must advect with the background flow on average. This legitimizes the common practice at Jicamarca and elsewhere of estimating bulk zonal plasma drifts from interferometric measurements of the apparent scatterer motion. Another important assumption validated by radar imaging is that the lifetime of the scattering intensifications must be a significant fraction of their transit time through the beam.

[22] The Doppler shifts of the finely resolved scattering intensifications showed considerable spatial variability here despite the fact that the spread *F* event in question was in its decay phase. In simulation, intensifications were associated with vertically steepened structures at the leading edges of convecting density fluctuations. Individually, the Doppler shifts of the intensified scattering regions should give a good representation of the plasma convection speed in the compact regions of space they represent, the steepened structures being essentially zero-frequency waves in the plasma frame of reference. Representing extremes in both convection speed and plasma density, however, the compact, sparse scattering regions are not a representative sample of the bulk fluid flow, the sampling is not ergodic, and coarsely-averaged Doppler shift measurements cannot a priori be expected to be an accurate tracer of the background plasma convection. Bias may be expected, since enhancements and depletions with equal relative density fluctuations convect in opposite directions but with unequal speeds.

[23] **Acknowledgments.** The Jicamarca Radio Observatory is a facility of the Instituto Geofisíco del Perú operated with support from NSF cooperative agreement ATM-0432565 through Cornell University. We appreciate the help of the Jicamarca staff, particularly the operations group. The C/NOFS mission is supported by the Air Force Research Laboratory, the Department of Defense Space Test Program, the National Aeronautics and Space Administration (NASA), the Naval Research Laboratory, and the Aerospace Corporation.

References

Costa, E., and M. C. Kelley (1978), On the role of steepened structures and drift waves in equatorial spread *F*, *J. Geophys. Res.*, *83*, 4359.

de Paula, E. R., and D. L. Hysell (2004), The São Luís 30 MHz coherent scatter ionospheric radar: System description and initial results, *Radio Sci.*, *39*, RS1014, doi:10.1029/2003RS002914.

Huba, J. D., and S. L. Ossakow (1979), On the generation of 3-m irregularities during equatorial spread F by low-frequency drift waves, *J. Geophys. Res.*, *84*, 6697.

Huba, J. D., and S. L. Ossakow (1981), Physical mechanism of the lower-hybrid-drift instability in a collisional plasma, *J. Atmos. Terr. Phys.*, *43*, 775.

Hysell, D. L. (1998), Imaging coherent scatter radar studies of bottomside equatorial spread *F*, *J. Atmos. Sol. Terr. Phys.*, *60*, 1109.

Hysell, D. L., and J. D. Burcham (1998), JULIA radar studies of equatorial spread *F*, *J. Geophys. Res.*, *103*, 29,155.

Hysell, D. L., and J. L. Chau (2006), Optimal aperture synthesis radar imaging, *Radio Sci.*, *41*, RS2003, doi:10.1029/2005RS003383.

Hysell, D. L., and M. C. Kelley (1997), Decaying equatorial *F* region plasma depletions, *J. Geophys. Res.*, *102*, 20,007.

Kelley, M. C., G. Haerendel, H. Kappler, A. Valenzuela, B. B. Balsley, D. A. Carter, W. L. Ecklund, C. W. Carlson, B. Häusler, and R. Torbert (1976), Evidence for a Rayleigh-Taylor type instability and upwelling of depleted density regions during equatorial spread *F*, *Geophys. Res. Lett.*, *3*, 448.

Kelley, M. C., et al. (1986), The Condor equatorial spread *F* campaign: Overview and results of the large-scale measurements, *J. Geophys. Res.*, *91*, 5487.

Mendillo, M., and A. Tyler (1983), Geometry of depleted plasma regions in the equatorial ionosphere, *J. Geophys. Res.*, *88*, 5778.

Morse, F. A., et al. (1977), Equion, an equatorial ionospheric irregularity experiment, *J. Geophys. Res.*, *82*, 578.

Otsuka, Y., K. Shiokawa, T. Ogawa, T. Yokoyama, M. Yamamoto, and S. Fukao (2004), Spatial relationship of equatorial plasma bubbles and field-aligned irregularities observed with an all-sky airglow imager and the Equatorial Atmosphere Radar, *Geophys. Res. Lett.*, *31*, L20802, doi:10.1029/2004GL020869.

Patra, A. K., S. Sripathi, and D. Tiwari (2004), Coupling effect of the equatorial F region irregularities on the low latitude E region instability processes, *Geophys. Res. Lett.*, *31*, L17803, doi:10.1029/2004GL020486.

Pfaff, R. F., J. H. A. Sobral, M. A. Abdu, W. E. Swartz, J. W. LaBelle, M. F. Larsen, R. A. Goldberg, and F. J. Schmidlin (1997), The Guará Campaign: A series of rocket-radar investigations of the Earth's upper atmosphere at the magnetic equator, *Geophys. Res. Lett.*, *24*, 1663.

Rino, C. L., R. T. Tsunoda, J. Petriceks, R. C. Livingston, M. C. Kelley, and K. D. Baker (1981), Simultaneous rocket-borne beacon and in situ measurements of equatorial spread *F*: Intermediate wavelength results, *J. Geophys. Res.*, *86*, 2411.

Tsunoda, R. T. (1983), On the generation and growth of equatorial b backscatter plumes: 2. Structuring of the west walls of upwellings, *J. Geophys. Res.*, *88*, 4869.

Tsunoda, R. T., and W. L. Ecklund (2007), On the post-sunset rise of the equatorial F layer and superposed upwellings and bubbles, *Geophys. Res. Lett.*, *34*, L04101, doi:10.1029/2006GL028832.

Tsunoda, R. T., R. C. Livingston, J. P. McClure, and W. B. Hanson (1982), Equatorial plasma bubbles: Vertically elongated wedges from the bottomside *F* layer, *J. Geophys. Res.*, *87*, 9171.

Woodman, R. F. (1960), Irregular refraction of satellite signals observed at Ancon, Peru, technical report, Inst. Geofis. del Perú, Lima.

Woodman, R. F. (2009), Spread *F*—An old equatorial aeronomy problem finally resolved?, *Ann. Geophys.*, *27*, 1915.

Woodman, R. F., and C. La Hoz (1976), Radar observations of *F* region equatorial irregularities, *J. Geophys. Res.*, *81*, 5447.

Yokoyama, T., S. Fukao, and M. Yamamoto (2004), Relationship of the onset of equatorial F region irregularities with the sunset terminator observed with the Equatorial Atmosphere Radar, *Geophys. Res. Lett.*, *31*, L24804, doi:10.1029/2004GL021529.

Zalesak, S. T., S. L. Ossakow, and P. K. Chaturvedi (1982), Nonlinear equatorial spread *F*: The effect of neutral winds and background Pedersen conductivity, *J. Geophys. Res.*, *87*, 151.

J. L. Chau and F. R. Galindo, Jicamarca Radio Observatory, Apartado 13-0207, Lima 13, Peru.

R. B. Hedden and D. L. Hysell, Department of Earth and Atmospheric Sciences, Cornell University, 2122 Snee Hall, Ithaca, NY 14853, USA. (dlh37@cornell.edu)

R. F. Pfaff, NASA Goddard Space Flight Center, Mail Code 696, Greenbelt, MD 20771, USA.

P. A. Roddy, Space Vehicles Directorate, Air Force Research Laboratory, 29 Randolph Road, Hanscom AFB, MA 01731, USA.